

Catalytic conversion of carbon dioxide into cyclic carbonates by Cu(II) and Ni(II) acetylacetonates anchored onto Siral 80

Senem COŞKUN¹, Zeynep TAŞCI², Mahmut ULUSOY³, Mürüvvet YURDAKOÇ^{1,*}

¹Department of Chemistry, Faculty of Science, Dokuz Eylül University, İzmir, Turkey

²Department of Chemistry, Faculty of Science, Muğla University, Muğla, Turkey

³Department of Chemistry, Faculty of Arts and Sciences, Harran University, Şanlıurfa, Turkey

Received: 14.08.2013 • Accepted: 08.01.2014 • Published Online: 11.06.2014 • Printed: 10.07.2014

Abstract: Ni and Cu acetylacetonates were anchored onto Siral 80 and used in the catalytic conversion of carbon dioxide. The catalysts were characterized by several methods such as XRD, FTIR, SEM, and TGA/DTG. The catalytic domains of the prepared heterogeneous complexes and their homogeneous counterparts were examined for the conversion reaction of carbon dioxide into cyclic carbonates in the presence of different additives (1.5 MPa CO₂ pressure, 100 °C, and 2 h). Good to excellent conversions were observed using Siral 80/APTES/Cu(acac)₂ catalysts and butylmethylimidazolium hexafluorophosphate, [bmim]PF₆, ionic liquid from the reaction of CO₂, and different epoxides. Modification with APTES made the immobilized metal complexes more efficient catalysts compared to their homogeneous counterparts and supporting material.

Key words: Siral 80, metal acetylacetonate, carbon dioxide, cyclic carbonate

1. Introduction

There is considerable interest in immobilization of reagents and homogeneous catalysts on organic or inorganic supports. The most often used method for anchoring different metal complexes on supports is the modification of the surface first with a suitable ligand. In recent years, especially within the concept of green chemistry, the anchoring of transition metal complexes onto solid supports or organic polymers has been an important research subject. In fact, these types of catalysts are used in heterogeneous catalytic reactions because of their structural selectivity; they also have several advantages in catalytic reactions, such as catalyst separation after the reaction and reusability in subsequent cycles/reactions.^{1–3}

The amount of atmospheric carbon dioxide has been above 350 ppm since 1988, which was determined as the upper safety limit by the NASA-Goddard Institute for Space Science (www.co2now.org). The amount of carbon dioxide has been increasing each year; hence it is the root of many problems, especially global warming. For the solution of these problems, in addition to the quest for alternative energy sources, many studies are being conducted on the storage of carbon dioxide and its conversion into valuable chemicals. Many value-added chemicals such as methanol, polycarbonate, and organic carbonates can be produced using carbon dioxide as a carbon source. Cyclic carbonates having a high boiling point, low toxicity, high solubility, and biodegradability have an important market as aprotic polar solvents and intermediates for fine chemical synthesis. Many catalysts such as ionic liquids,^{4,5} quaternary ammonium and phosphonium salts,^{6–8} metal

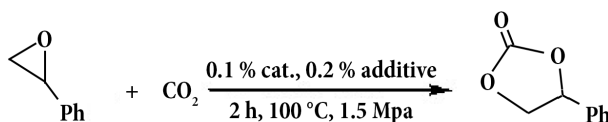
*Correspondence: m.yurdakoc@deu.edu.tr

complexes,^{9–14} alkali metal salts,^{15–17} metal oxides,^{18–21} cellulose/KI,²² ion exchange resins,²³ metal organic frameworks,^{24–26} and heterogeneous systems,^{27–32} have been developed for the cycloaddition reaction of CO₂ and epoxides.

The metal acetylacetonates are easily accessible and relatively inexpensive complexes. They have been extensively used in various homogeneous reactions such as epoxidation, esterification, and benzylation of various alcohols using *tert*-butylhydroperoxide (*t*-BuOOH), butyric acid, and benzyl chloride.^{33–35} The catalytic activity of metal acetates in the presence of tetraethyl ammonium bromide has been examined recently.³⁶

It has also been reported that heterogeneous catalysts that are capable of anchoring different transition metal compounds may be prepared stepwise, first by modifying the support material with aminopropyltriethoxysilane (APTES), then by utilizing the gas–solid reactions under reflux conditions, and finally immobilization of transition metal acetylacetonates onto these modified supports.^{37–42}

In the present study, heterogeneous catalysts were prepared by using Siral 80 as a support material, APTES as a modifier, and Cu(acac)₂ or Ni(acac)₂ as metal acetylacetonates according to the procedure explained above, and characterized. The catalysts were tested for the chemical fixation of carbon dioxide according to the model reaction in Scheme 1.



Scheme. Cycloaddition reaction of carbon dioxide and epoxides.

2. Experimental

2.1. Materials, reagents, solvents, and measurements

Siral 80 was obtained from SASOL-Condea AG, Germany. The chemical composition of Siral 80 is 78.3% SiO₂, 21.7% Al₂O₃, 0.02% Fe₂O₃, 0.02% TiO₂, 0.01% CaO, and 0.2% MgO. Particle size distribution as percentages in the ranges <25 μm, <45 μm, and <90 μm is 73.3, 96.2, and 98.7, respectively.^{43,44} The compounds (3-aminopropyl) triethoxysilane (APTES), copper(II) and nickel acetylacetonates, dry toluene, glycerol, and benzyl chloride were purchased from Aldrich, while chloroform was from Merck, and they were used without any purification.

2.2. Preparation of the catalysts

2.2.1. Direct anchoring of metal(II) acetylacetonate onto support material (method A)

A solution of M(acac)₂ (90 μmol) in chloroform (50 mL) was refluxed with Siral 80 (0.60 g) for 24 h. The resulting solid was filtered and refluxed again with chloroform (50 mL) for 2 h. It was recovered by vacuum filtration and then dried in an oven at 110 °C for 3 h. These materials will be labeled as Siral 80/M(acac)₂.

2.2.2. Functionalization of support material with (3-aminopropyl)triethoxysilane (APTES) (method B)

The catalysts were prepared according to the procedure of Pereira et al.^{41,42} as detailed below. The support material was heated in an oven at 120 °C for 1 h. Afterwards, Siral 80 (2.00 g) in dry toluene (100 mL) and 1.18 mL of APTES (5.06 mmol) were refluxed for 24 h. The resulting material was filtered by vacuum, refluxed

with dry toluene (100 mL) for 2 h, and then dried in a vacuum oven at 120 °C for 3 h. These materials will be referred to as Siral 80/APTES.

2.2.3. Anchoring of copper(II) and nickel(II) acetylacetonates onto APTES-functionalized support material

A solution of $\text{Cu}(\text{acac})_2$ or $\text{Ni}(\text{acac})_2$ (0.0236 g) in chloroform (50 mL) was refluxed with Siral 80/APTES (0.60 g) for 24 h. The resulting solids were filtered by vacuum, refluxed with chloroform (50 mL) for 2 h, recovered by vacuum filtration, and then dried in an oven at 110 °C for 3 h under vacuum. These materials will be referred to as Siral 80/APTES/ $\text{M}(\text{acac})_2$.

2.3. Physicochemical measurements

The bulk copper and nickel contents were determined by atomic absorption spectroscopy in a PerkinElmer SP9 spectrometer. Samples (20 mg) were previously dried at 100 °C, and mixed with aqua regia (2 mL) and HF (3 mL) for 2 h at 120 °C in a stainless-steel autoclave equipped with a polyethylene-covered beaker (ILC B240). After cooling to room temperature, the solution was mixed with boric acid (about 2 g) and finally adjusted to a known volume with deionized water. The AAS analysis results for copper and nickel contents of the samples are given in Table 1.

Table 1. Amount of metal ions on support materials analyzed by AAS.

| Material | Metal amount |
|--|----------------------------------|
| | (μg metal/g support) |
| Siral 80/APTES/ $\text{Cu}(\text{acac})_2$ | 1900 |
| Siral 80/ $\text{Cu}(\text{acac})_2$ | 6050 |
| Siral 80/APTES/ $\text{Ni}(\text{acac})_2$ | 2825 |
| Siral 80/ $\text{Ni}(\text{acac})_2$ | 9175 |

These catalysts and supports were characterized by different methods. X-ray powder diffraction (XRD) patterns of the samples were determined by using a Rigaku D_{max} 2200/PC model instrument with $\text{Cu}K_{\alpha}$ radiation (40 kV, 40 mA).

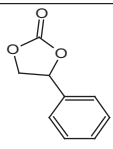
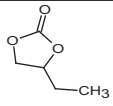
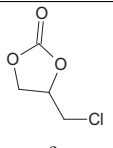
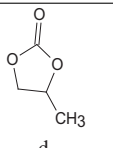
Brunauer–Emmett–Teller (BET) specific surface area (S_{BET}) values of the samples were obtained from N_2 adsorption–desorption isotherms at 77 K, measured on a SORPTOMATIC 1990 after degassing under vacuum for 3 h at 150 °C by using MILES-200 Advanced Data Processing Sorption Software Version 3.00. S_{BET} values were as follows: for Siral 80: 224, for Siral 80/APTES/ $\text{Cu}(\text{acac})_2$: 77, and for Siral 80/APTES/ $\text{Ni}(\text{acac})_2$: 65 $\text{m}^2 \text{g}^{-1}$.

Infrared spectra were recorded by means of a PerkinElmer FT-IR spectrophotometer (Spectrum BX-II) in the range 4000–400 cm^{-1} in KBr disks. Each disk was prepared by careful grinding of the KBr (90 mg) with the samples (0.9 mg). Thermogravimetric (TG) analysis of the samples was carried out with a PerkinElmer Diamond TG/DTA Analyzer using Pt pans in the temperature range 30–1000 °C with a heating rate of 10 °C/min. TG analysis was performed on the dried samples with a heating rate of 10 °C/min and under a stream of nitrogen gas (flow rate: 50 mL/min). SEM micrographs were performed with a scanning electron microscope, Jeol JSM 60, operating at an accelerating voltage of 20 kV. The samples were dried before gold sputter-coating for SEM analysis. SEM images were taken at different magnifications (between 1000 \times and 10,000 \times).

2.4. General procedure for the cycloaddition of epoxides and CO₂

Catalytic tests were performed in a PARR 4843 50-mL stainless steel pressure reactor. In a typical reaction, immobilized metal acetylacetonate compound, (1.125×10^{-5} mol), epoxide (1.3 mL, 1.125×10^{-2} mol), and DMAP (2.75 mg, 2.25×10^{-5} mol) were charged into the reactor under solventless conditions. The reaction pressure of carbon dioxide was set to 15 atm and the temperature of the reactor vessel was held at 100 °C during the reaction. After expiration of the reaction time, the vessel was cooled to 5–10 °C in an ice bath. To reduce the pressure, the excess gases were vented out. The conversions of epoxides to corresponding cyclic carbonates were determined by comparing the ratio of product to substrate in the ¹H NMR spectrum of an aliquot of the reaction mixture. Coupling of CO₂, various epoxides catalyzed by Siral 80/APTES/Cu(acac)₂, and ¹H NMR data of the products (defined as a, b, c, and d) are shown in Table 2.

Table 2. Coupling of CO₂ and various epoxides catalyzed by Siral 80/APTES/Cu(acac)₂.

| Entry | Product | Yield (%) | TON | TOF(h ⁻¹) |
|-------|--|-----------|-----|-----------------------|
| 1 |  a | 92 | 920 | 460 |
| 2 |  b | 50 | 500 | 250 |
| 3 |  c | 99 | 990 | 495 |
| 4 |  d | 67 | 670 | 335 |

Reaction conditions: cat. (1.125×10^{-5} mol), [bmim]PF₆ (2.25×10^{-5} mol), epoxide (1.125×10^{-2} mol), CO₂ (1.5 MPa), 100 °C, 2 h.

¹H NMR data of the products:

a) Styrene carbonate: δ H(CDCl₃) 4.35 (1H, dd, $J = 8.5$ Hz, $J = 8.0$ Hz, OCH₂), 4.81 (1H, dd, $J = 8.5$ Hz, $J = 8.0$ Hz, OCH₂), 5.68 (1H, t, $J = 8.0$ Hz, PhCHO), 7.2–7.5 (5H, m, ArH); δ C(CDCl₃) 71.3, 78.1, 126.0, 129.3, 129.8, 135.9, 154.9.

b) 1,2-butene carbonate: δ 1.03 (3H, t, $J = 7.6$ Hz, CH₃), 1.75–1.86 (2H, m, CH₂), 4.11 (1H, dd, $J = 8.4$, $J = 6.8$ Hz, OCH₂), 4.55 (1H, dd, $J = 8.4$ Hz, $J = 7.6$, OCH₂), 4.66–4.73 (1H, m, CH).

c) Chloromethyl ethylene carbonate: δ H(CDCl₃) 3.3–3.8 (2H, m, CH₂Cl), 4.40 (1H, dd, $J = 8.9$, 8.7 Hz, OCH₂), 4.59 (1H, dd, $J = 8.9$, 8.4 Hz, OCH₂), 4.9–5.0 (1H, m, OCH); δ C(CDCl₃) 43.9, 67.4, 74.6, 154.4.

d) Propylene carbonate: δ H(CDCl₃) 1.49 (3H, d, $J = 6.3$ Hz, CH₃), 4.02 (1H, dd, $J = 8.4$, 7.3 Hz, OCH₂), 4.55 (1H, dd, $J = 8.4$ Hz, $J = 8.0$, OCH₂), 4.8–4.9 (1H, m, CHO); δ C(CDCl₃) 19.7, 70.9, 73.7, 154.1.

3. Results and discussion

3.1. Characterization of the catalysts

X-ray diffraction patterns and data of the samples are given in Figure 1 and Table 3, respectively.

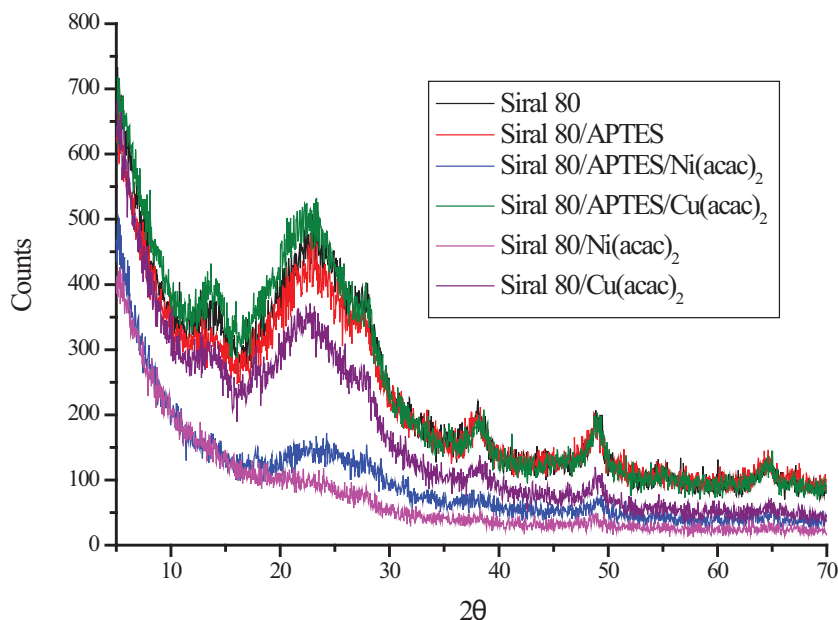


Figure 1. X-ray diffraction patterns of the samples.

In the diffraction patterns of all samples, the XRD pattern of Siral 80 was still observed. However, the signal intensities of the peaks decreased in general. The XRD peak signals of Siral 80/APTES/Cu(acac)₂ were the highest, while the minimum was observed in the case of Siral 80/Ni(acac)₂. On the other hand, the basal spacing (d_{001}) of the samples was increased by 1.53 Å as compared with Siral 80 in the case of Siral 80/APTES/Ni(acac)₂. The basal spacing values for Siral 80, Siral 80/APTES, Siral 80/APTES/Cu(acac)₂, and Siral 80/APTES/Ni(acac)₂ were determined as 6.29 Å, 6.88 Å, 6.58 Å, and 7.82 Å, respectively. In the case of direct modification of Siral 80 with Cu and Ni(acac)₂, 6.89 and 6.50 Å values were obtained for Siral 80/Cu(acac)₂ and Siral 80/Ni(acac)₂, respectively.

Table 3. XRD data of Siral 80 supported catalysts.

| Sample | [$^{\circ}2\theta$] | d-spacings [Å] |
|--------------------------------------|-----------------------------------|------------------------------|
| Siral 80 | 14.08; 22.70; 27.98; 38.17; 48.99 | 6.29; 3.92; 3.19; 2.35; 1.86 |
| Siral 80/APTES | 12.87; 22.80; 27.56; 38.01; 48.70 | 6.88; 3.90; 3.24; 2.37; 1.87 |
| Siral 80/Cu(acac) ₂ | 12.83; 18.18; 28.86; 49.41; 51.96 | 6.89; 4.88; 3.09; 1.84; 1.76 |
| Siral 80/Ni(acac) ₂ | 13.60; 21.42; 26.42 | 6.50; 4.15; 3.37 |
| Siral 80/APTES/Cu(acac) ₂ | 13.46; 28.07; 38.34; 48.98 | 6.58; 3.18; 2.35; 1.86 |
| Siral 80/APTES/Ni(acac) ₂ | 11.32; 20.92; 24.22 | 7.82; 4.25; 3.67 |

FT-IR spectra of the samples are given in Figure 2. The FT-IR spectra of Siral 80 and the other samples contained a broad band corresponding to -OH stretching at 3443 cm⁻¹. The band at around 1660 or 1649 cm⁻¹ also corresponds to the -OH deformation (bending) of adsorbed water. The strong bands at 1076 or 1078 and

around 786 cm^{-1} are due to $\nu_{asym}(\text{Si-O})$ and $\nu_{sym}(\text{Si-O})$ of the Cu-Ni/Siral 80 skeleton, respectively. The bands at around 938 cm^{-1} are attributed to M-OH bending vibration deformation bands. The Si-O stretching vibrations were observed at 780 cm^{-1} and 635 cm^{-1} in Siral 80/APTES/Cu(acac)₂. These reflected the presence of silica and quartz. The bands at $459\text{--}468\text{ cm}^{-1}$ correspond to Si-O-Si bending vibrations in Siral 80 samples.⁴⁵

After APTES grafting onto Siral 80, there were no practical changes in band shapes for Siral 80/APTES. The broad band centered at around 3429 cm^{-1} is an envelope of ν_{O-H} for adsorbed water, silanol groups, and ν_{N-H} of the amino groups. No band due to $-\text{NH}_2$ stretching could be observed, as it was masked by the broad $-\text{OH}$ bending band. In the case of copper and nickel acetylacetonates anchored onto Siral 80/APTES, the $-\text{CH}_2$ stretching vibration band from APTES at 2918 cm^{-1} still appeared as can be seen at 2928 and 2921 cm^{-1} in the case of Cu(acac)₂ and Ni(acac)₂, respectively. The band for aliphatic $-\text{C}=\text{C}-$ stretching vibrations from Cu(acac)₂ and Ni(acac)₂ at $1500\text{--}1600\text{ cm}^{-1}$ was also observed. The band due to $-\text{NH}_2$ was not detected. C-N bending vibration bands were seen at 1260 and 1274 cm^{-1} . The weak broad band at around 1536 cm^{-1} for $-\text{C}-\text{O}-$ in Cu(acac)₂ and at 1520 cm^{-1} for Ni(acac)₂ samples was also observed.⁴⁵ FT-IR spectra of the samples reflect mainly the FT-IR spectrum of Siral 80.

TGA/DTG data of the samples are given in Table 4. In the TGA/DTG data of Siral 80/APTES, the removal of adsorbed water with a mass loss was 10.37% was observed in the first stage, $25\text{--}200\text{ }^\circ\text{C}$. On the other hand, in the TGA/DTG profiles of the samples, the second and third stage mass losses showed the same amount of decay corresponding to the decomposition of APTES species. Finally, the last mass losses occurred in the temperature range $500\text{--}1000\text{ }^\circ\text{C}$, which might be attributed to evolution of the adsorbed water due to the dehydroxylation of surface $-\text{OH}$ groups of SiO_2 between the layers of catalysts. The total mass losses were

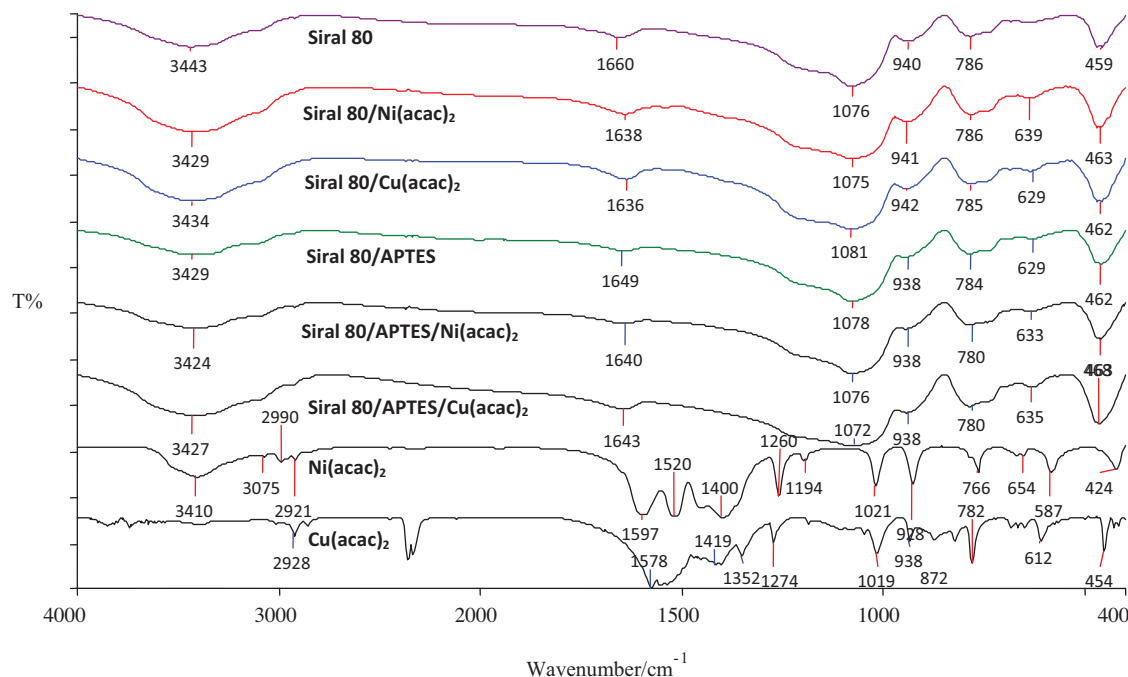


Figure 2. FT-IR spectra of the samples.

18.98%, 20.07%, 19.57%, and 12.74% for Siral 80, Siral 80/APTES, Siral 80/APTES/Cu(acac)₂, and Siral 80/APTES/Ni(acac)₂, respectively. In the case of Siral 80, Siral 80/Cu(acac)₂, and Siral 80/Ni(acac)₂, the total mass losses were 18.98%, 20.89%, and 15.4%, respectively. The mass loss in the case of Siral 80/Ni(acac)₂ was less than that of Siral 80/Cu(acac)₂ and 3 mass loss stages were observed. The dehydration of Siral 80 occurred with a mass loss of 12.70% in the temperature range 25–230 °C as a single-step process, which gave rise to an endothermic maximum at 85 °C due to the physically adsorbed water. A second mass loss occurred at temperatures in the range 230–1000 °C, where the TGA/DTG curve displayed a steep mass loss (about 6.28%) related to the release of H₂O from structural –OH (dehydroxylation) of synthetic Siral 80.

SEM images of the samples are given in Figures 3a–f. The SEM images of Siral 80 and Siral 80-based samples reflected in general the surface morphology of small, medium-sized, and large spherical grains. The size of the particles can be calculated from the scale on the image as of the order of 10 μm.

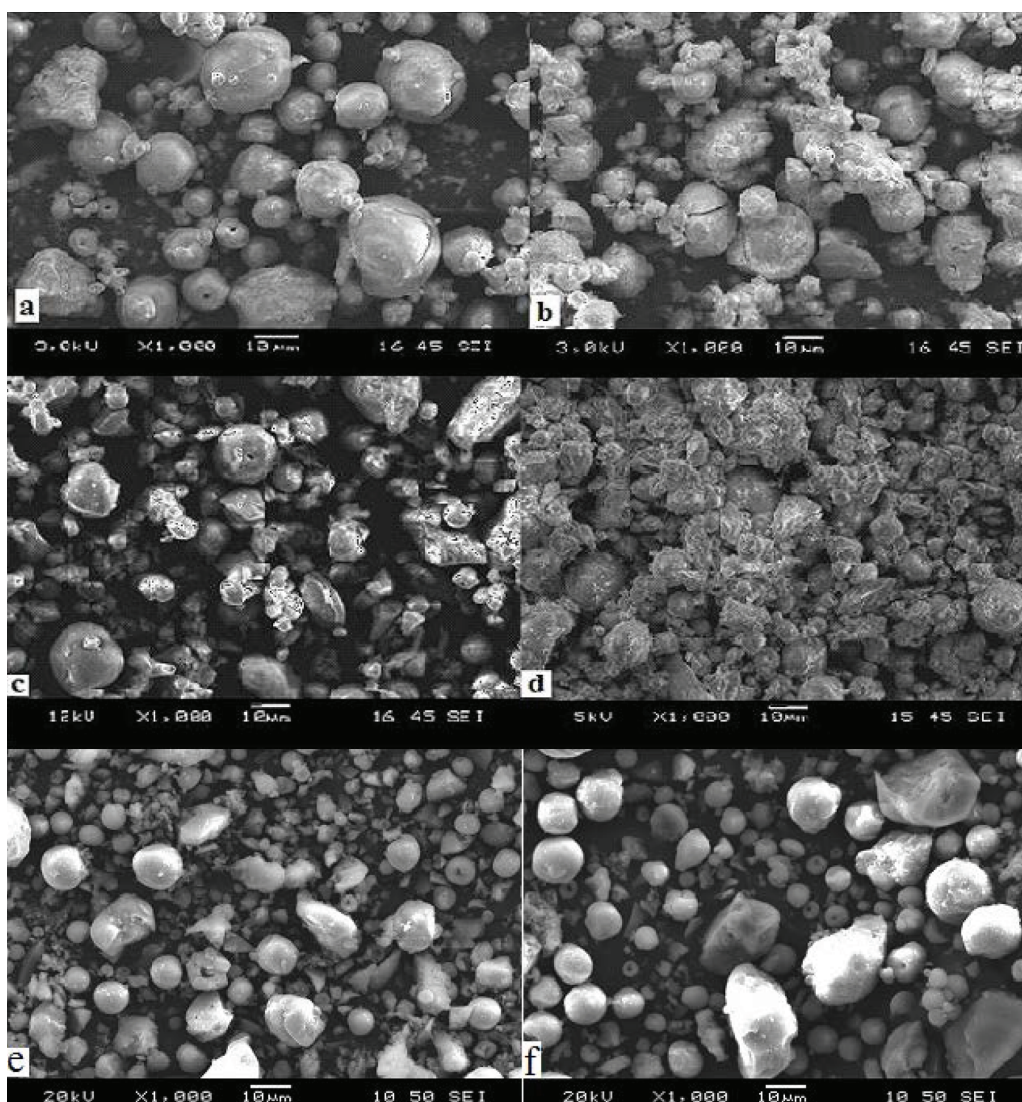


Figure 3. SEM images of the samples: a) Siral 80, b) Siral 80/APTES, c) Siral 80/APTES/Cu(acac)₂, d) Siral 80/Cu(acac)₂, e) Siral 80/Ni(acac)₂, f) Siral 80/APTES/Ni(acac)₂.

Table 4. TGA/DTG data of the samples.

| Sample | Step 1 T.R. (°C)/Mass loss (%) | Step 2 T.R. (°C)/Mass loss (%) | Step 3 T.R. (°C)/Mass loss (%) | Step 4 T.R. (°C)/Mass loss (%) |
|--------------------------------------|--------------------------------------|--------------------------------------|--------------------------------------|--------------------------------------|
| Siral 80 | 25–230/12.70 | 230–1000/6.28 | – | – |
| Siral 80/APTES | 25–200/10.37 | 200–300/1.89 | 300–510/5.78 | 500–1000/2.03 |
| Siral 80/Cu(acac) ₂ | 25–200/12.94 | 200–325/1.75 | 325–523/4.50 | 523–1000/1.70 |
| Siral 80/Ni(acac) ₂ | 25–215/8.8 | 215–552/5.00 | – | 552–1000/1.60 |
| Siral 80/APTES/Cu(acac) ₂ | 25–175/7.31 | 195–320/2.92 | 320–510/5.88 | 510–1000/3.26 |
| Siral 80/APTES/Ni(acac) ₂ | 25–200/6.7 | 213–312/0.88 | 312–510/4.26 | 510–1000/0.90 |

T.R.: Temperature range.

The evaluation of the SEM images of the Siral-based samples reflected the main structure of Siral 80 (Figure 3a); this means spherical grains of various sizes. After treatment with APTES (Figure 3b) and Cu(acac)₂ (Figure 3d), coagulation of the APTES and Cu(acac)₂ particles onto the surface of the Siral 80 was observed. The stepwise treatment increased the condensation of the particles (tiny sticky particles) around the spherical grains of Siral 80. In the case of Siral 80/APTES/Ni(acac)₂, the SEM image is somewhat different (see Figures 3c and d) such that one cannot see any coagulation around the Siral 80 grains. Particles around the large spherical grains are observed for Siral 80/Ni(acac)₂ (Figure 3e) and larger spherical grains for Siral 80/APTES/Ni(acac)₂ in Figure 3f.

3.2. Catalytic properties

According to the generally accepted mechanism for the cycloaddition reaction of carbon dioxide and epoxides, a Lewis acid and a Lewis base are required. The Lewis base opens the epoxide ring via a nucleophilic attack, which leads to an oxy anion species bonding a Lewis acidic metal center; then cyclic carbonate forms after reacting with CO₂.^{27–31} Catalytic experiments were carried out at optimized conditions, which were determined in previous studies.²⁷ Catalytic efficiencies of heterogeneous metal complexes for the cycloaddition reaction of CO₂ were evaluated using an additive (DMAP, NBu₄Br, or bmimPF₆) as a Lewis base (Table 5). When using only heterogeneous metal complexes we did not detect any catalytic conversion (Table 5, entries 5 and 6). Control reactions using homogeneous Cu(acac)₂ and Ni(acac)₂ were also conducted, which gave 3% and 4% conversions, respectively. In contrast, immobilized catalysts dramatically increased the yield up to 75% under the same conditions. Similar behavior was reported by several authors.^{28–31} This difference in catalytic activity should be explained by the structure of the solid support materials. We supposed that pore size, surface area, and –OH groups on the surface of the supporting material were the main parameters.^{5,7,46} The catalytic activities of the heterogeneous catalyst were found in the following order: Siral 80 < Siral 80/APTES. Modification with APTES increased the catalytic activity. Kumar has recently reported that different metal acac compounds were efficient as catalysts (50 °C, 50 bar CO₂ pressure, 4.5 h) using 1 mol % catalyst and NEt₄Br.³⁶

Instead of DMAP, tetrabutylammonium bromide (NBu₄Br) and butylmethylimidazolium hexafluorophosphate (bmimPF₆) were applied as an additive to Siral 80/APTES/Cu(acac)₂ catalysts. Conversion of styrene oxide was found to increase in the order of DMAP < NBu₄Br < [bmim]PF₆.

The applicability of the catalytic system to other terminal epoxides was examined (Table 2). The catalyst system Siral 80/APTES/Cu(acac)₂/[bmim]PF₆ was found to be feasible with various epoxides that have both

Table 5. Conversion of styrene oxide to styrene carbonate.^a

| Entry | Catalyst | Additive | Conv. (%) | TOF (h ⁻¹) |
|-------|--------------------------------------|-----------------------|-----------|------------------------|
| 1 | Siral 80/APTES/Cu(acac) ₂ | DMAP | 75 | 375 |
| 2 | Siral 80/Cu(acac) ₂ | DMAP | 60 | 300 |
| 3 | Siral 80/APTES/Ni(acac) ₂ | DMAP | 72 | 360 |
| 4 | Siral 80/Ni(acac) ₂ | DMAP | 53 | 265 |
| 5 | Siral 80/APTES/Cu(acac) ₂ | - | - | 0 |
| 6 | Siral 80/APTES/Ni(acac) ₂ | - | - | 0 |
| 7 | Cu(acac) ₂ | DMAP | 3 | 15 |
| 8 | Ni(acac) ₂ | DMAP | 4 | 20 |
| 9 | Siral 80/APTES/Cu(acac) ₂ | NBu ₄ Br | 82 | 410 |
| 10 | Siral 80/APTES/Ni(acac) ₂ | NBu ₄ Br | 80 | 300 |
| 11 | Siral 80/APTES/Cu(acac) ₂ | [bmim]PF ₆ | 92 | 460 |
| 12 | Siral 80/APTES/Ni(acac) ₂ | [bmim]PF ₆ | 89 | 375 |
| 13 | — | DMAP | 5 | 25 |
| 14 | — | [bmim]I | 14 | 70 |
| 15 | — | NBu ₄ Br | 25 | 125 |
| 16 | — | [bmim]PF ₆ | 52 | 260 |

^a Reaction conditions: cat. (1.125×10^{-5} mol), styrene oxide (1.125×10^{-2} mol, 1.3 mL), additive (2.25×10^{-5} mol), 100 °C, 2 h, 1.5 MPa.

electron-withdrawing and electron-donating substituents. The conversion of epichlorohydrine is the highest, which is presumably due to having electron-withdrawing capability. For each reaction, cyclic carbonates were formed exclusively.

The reusability of Siral 80/APTES/Cu(acac)₂ was examined. The efficiency of the catalyst decreased suddenly after a second use (92%, 80%, and 20%). This indicates that the metal complex is only weakly bound to the supporting material and rapid leaching has occurred during the catalytic reaction.

4. Conclusion

The catalytic domains of the prepared heterogeneous complexes and their homogeneous counterparts were examined for the conversion reaction of carbon dioxide into cyclic carbonates in the presence of different additives (1.5 MPa CO₂ pressure, 100 °C, and 2 h). It was found that while homogeneous Cu(acac)₂ and Ni(acac)₂ did not show any catalytic domains, their Siral 80 immobilized derivatives exhibited notable conversion efficiency. Good to excellent conversions were observed using Siral 80/APTES/Cu(acac)₂ catalyst and [bmim]PF₆ with the reaction of CO₂ and different epoxides. It is unfortunate, however, that this catalyst system is not a good heterogeneous one due to sudden reduction in the conversion after the second usage.

Acknowledgments

This work has been supported by TÜBİTAK (106T364 and 110T655) and ÖYP (2005DPT003/7). The authors are also grateful to the Research Foundation of Dokuz Eylül University (2012.KB.FEN.035) for the financial support.

References

1. Valkenberg, M. H.; Hölderich, W. F. *Catal. Rev.* **2002**, *44*, 321–374.
2. Corma, A.; Garcia, H. *Adv. Synth. Catal.* **2006**, *348*, 1391–1412.
3. Dooos, B. M. L.; Vankelecom, I. F. J.; Jacobs, P. A. *Adv. Synth. Catal.* **2006**, *348*, 1413–1446.
4. Motokura, K.; Itagaki, S.; Iwasawa, Y.; Miyaji, A.; Baba, T. *Green Chem.* **2009**, *11*, 1876–1880.
5. Sun, J.; Zhang, S.; Cheng, W.; Ren, J. *Tetrahedron Lett.* **2008**, *49*, 3588–3591.
6. He, T.; Wu, J.; Zhang, Z.; Ding, K.; Han, B.; Xie, Y.; Jiang, T.; Liu, Z. *Chem. Eur. J.* **2007**, *13*, 6992–6997.
7. Sun, J.; Ren, J.; Zhang, S.; Cheng, W. *Tetrahedron Lett.* **2009**, *50*, 423–426.
8. Zhao, Y.; Tian, J. S.; Qi, X. H.; Han, Z. N.; Zhang, Y. Y.; He, L. N. *J. Mol. Catal. A* **2007**, *271*, 284–289.
9. Chang, T.; Jin, L.; Jing, H. *ChemCatChem* **2009**, *1*, 379–383.
10. Decortes, A.; Castilla, A. M.; Kleij, A. W. *Angew. Chem. Int. Ed.* **2010**, *49*, 9822–9837.
11. Taşçı, Z.; Kunduracıoğlu, A.; Kani, İ.; Çetinkaya, B. *ChemCatChem* **2012**, *4*, 831–835.
12. Yasuda, H.; He, L. N.; Sakakura, T. *J. Catal.* **2002**, *209*, 547–550.
13. Buchard, A.; Kember, M. R.; Sandeman, K. G.; Williams, C. K. *Chem. Comm.* **2011**, *47*, 212–214.
14. Man, M. L.; Lam, K. C.; Sit, W. N.; Ng, S. M.; Zhou, Z.; Lin, Z.; Lau, C. P. *Chem. Eur. J.* **2006**, *12*, 1004–1015.
15. Song, J.; Zhang, Z.; Hu, S.; Wu, T.; Jiang, T.; Han, B. *Green Chem.* **2009**, *11*, 1031–1036.
16. Ramidi, P.; Munshi, P.; Gartia, Y.; Pulla, S.; Biris, A. S.; Paul, A.; Ghosh, A. *Chem. Phys. Lett.* **2011**, *512*, 273–277.
17. Srivastava, R.; Bennur, T. H.; Srinivas, D. *J. Mol. Catal. A: Chem.* **2005**, *226*, 199–205.
18. Yamaguchi, K.; Ebitani, K.; Yoshida, T.; Yoshida, H.; Kaneda, K. *J. Am. Chem. Soc.* **1999**, *121*, 4526–4527.
19. Srivastava, R.; Srinivas, D.; Ratnasamy, P. *J. Catal.* **2005**, *233*, 1–15.
20. Murugan, C.; Sharma, S. K.; Jasra, R. V.; Bajaj, H. C. *Ind. J. Chem.* **2010**, *49A*, 288–294.
21. Ramin, M.; Vegten, N.; Grunwaldt, J. D.; Baiker, A. *J. Mol. Catal. A* **2006**, *258*, 165–171.
22. Liang, S.; Liu, H.; Jiang, T.; Song, J.; Yang, G.; Han, B. *Chem. Commun.* **2011**, *47*, 2131–2133.
23. Du, Y.; Cai, F.; Kong, D. L.; He, L. N. *Green Chem.* **2005**, *7*, 518–523.
24. Macias, E. E.; Ratnasamy, P.; Carreon, M. A. *Catal. Today* **2012**, *198*, 215–218.
25. Carreon, M. A. *In. J. Chem. A* **2012**, *51A*, 1306–1314.
26. Zhu, M.; Srinivas, D.; Bhogeswararao, S.; Ratnasamy, P.; Carreon, M. A. *Catal. Commun.* **2013**, *32*, 36–40.
27. Ulusoy, M.; Cetinkaya, E.; Cetinkaya, B. *Appl. Organomet. Chem.* **2009**, *23*, 68–74.
28. Sakai, T.; Tsutsumi, Y.; Ema, T. *Green Chem.* **2008**, *10*, 337–341.
29. Shiels, R. A.; Jones, C. W. *J. Mol. Catal. A* **2007**, *261*, 160–166.
30. Srivastava, R.; Srinivas, D.; Ratnasamy, P. *Tetrahedron Lett.* **2006**, *47*, 4213–4217.
31. Taşçı, Z.; Ulusoy, M. *J. Organomet. Chem.* **2012**, *713*, 104–111.
32. Udayakumar, S.; Lee, M. K.; Shim, H. L.; Park, S. W.; Park, D. W. *Catalysis Comm.* **2009**, *10*, 659–664.
33. Conte, V.; Di Furia, F.; Licini, G. *Appl. Catal. A General* **1997**, *157*, 335–361.
34. Bolm, C. *Coord. Chem. Rev.* **2003**, *237*, 245–256.
35. Ligtenbarg, A. G. J.; Hage, R.; Feringa, B. L. *Coord. Chem. Rev.* **2003**, *237*, 89–101.
36. Kumar, S.; Jain, S. L.; Sain, B. *Catal. Lett.* **2012**, *142*, 615–618.
37. Vansant, E. F.; van der Voort, P.; Vrancken, K. C. *Characterization and Chemical Modification of the Silica Surface, Studies in Surface Science and Catalysis*, Vol. 93, Elsevier, Amsterdam, 1995, pp. 149–192.

38. Haukka, S.; Lakomaa, E. L.; Suntola, T. *Thin Solid Films* **1993**, *225*, 280–283.
39. Lakomaa, E. L. *Appl. Surf. Sci.* **1994**, *75*, 185–196.
40. Haukka, S.; Kytökivi, A.; Lakomaa, E. -L.; Lehtovirta, U.; Lindblad, M.; Lujala, V.; Suntola, T. in: G. Poncelet, et al. (Eds.), *Preparation of Catalysts VI*, Elsevier, the Netherlands, 1995, p. 957.
41. Pereira, C.; Patrício, S.; Silva, A. R.; Magalhães, A. L.; Carvalho, A. P.; Pires, J.; Freire, C. *J. Colloid Int. Sci.* **2007**, *316*, 570–579.
42. Pereira, C.; Silva, A. R.; Carvalho, A. P.; Pires, J.; Freire, C. *J. Mol. Catal. A Chem* **2008**, *283*, 5–14.
43. Yurdakoç, M.; Akçay, M.; Tonbul, Y.; Yurdakoç, K. *Turk. J. Chem.* **1999**, *23*, 319–327.
44. Yurdakoç, M.; Seki, Y.; Karahan, S.; Yurdakoç, K. *J. Coll. Int. Sci.* **2005**, *286*, 440–446.
45. Daniell, W.; Schubert, U.; Glöckler, R.; Meyer, A.; Noweck, K.; Knözinger, H. *Applied Catal. A General* **2000**, *196*, 247–260.
46. Liang, S.; Liu, H.; Jiang, T.; Song, J.; Yang, G.; Han, B. *Chem. Commun.* **2011**, *47*, 2131–2133.